

# Ab-initio calculation of the vibrational modes of $\text{SiH}_4$ , $\text{H}_2\text{SiO}$ , $\text{Si}_{10}\text{H}_{16}$ , and $\text{Si}_{10}\text{H}_{14}\text{O}$

Katalin Gaál-Nagy, Giulia Canevari, and Giovanni Onida

European Theoretical Spectroscopy Facility (ETSF), CNR-INFM and Dipartimento di Fisica, Università degli Studi di Milano, via Celoria 16, I-20133 Milano, Italy

E-mail: katalin.gaal-nagy@physik.uni-regensburg.de

**Abstract.** We have studied the normal modes of hydrogenated and oxidized silicon nanocrystals, namely  $\text{SiH}_4$  (silan),  $\text{H}_2\text{SiO}$  (silanon),  $\text{Si}_{10}\text{H}_{16}$  and  $\text{Si}_{10}\text{H}_{14}\text{O}$ . The small clusters ( $\text{SiH}_4$  and  $\text{H}_2\text{SiO}$ ) have been used for convergence tests and their bondlengths and frequencies have been compared with experimental and theoretical reference data. For the large clusters ( $\text{Si}_{10}\text{H}_{16}$  and  $\text{Si}_{10}\text{H}_{14}\text{O}$ ) we have investigated the vibrational density of states where we have identified the oxygen-related spectral features. The vibrational modes have been also analyzed with respect to the displacement patterns. The calculations have been carried out within the density-functional and density-functional perturbation theory using the local-density approximation.

## 1. Introduction

Silicon nanostructures have important applications in microelectronics due to the downscaling of optoelectronic devices. Because of this, the optical, electronic, and vibrational properties of these systems are of large interest. For example, photoluminescence of quantum wires has been discovered [1]. The investigation of silicon nanocrystals is another step in the direction of the development of nanostructured devices. Although the electronic and optical properties of oxidized and non-oxidized nanocrystals have been studied extensively [2–6], much less is known about their vibrational properties. Nevertheless, the production and operation of devices is carried out at room temperature where the vibrations of the crystals play an important role. They can enhance adsorption processes as well as they can influence the optical properties of the systems.

$\text{Si}_{10}\text{H}_{16}$  and  $\text{Si}_{10}\text{H}_{14}\text{O}$  are good models for the study of (oxidized) miniaturized semiconductors, since they are simple and they can be studied with fully ab-initio total energy calculations. Thus, we have studied the vibrational properties for these systems as prototypes for non-oxidized and oxidized nanocrystals. Besides the influence of the dynamics of the nanocrystals to chemical processes, their vibrational frequencies can also be utilized for the characterization of the oxidized clusters due to the signature of the oxygen in the vibrational density of states. In a first step we have studied smaller systems (silan and silanon) to assess the numerical convergence. Furthermore, for silan and silanon experimental and theoretical reference data exist which can be used for comparison.

This article is organized as follows: after a short description of the method employed in our calculations, we present the results for silan and silanon (Sect. 3), where the convergence tests,

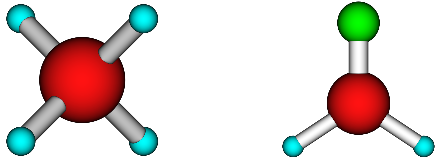


**Figure 1.** Silan (left) and silanon (right). Silicon atoms are drawn with large dark-red spheres, hydrogen atoms with small light-blue ones, and oxygen atoms with medium-sized green ones.

an analysis of the displacement patterns, and a comparison with experimental and theoretical results are shown. Then, we investigate  $\text{Si}_{10}\text{H}_{16}$  and  $\text{Si}_{10}\text{H}_{14}\text{O}$  (Sect. 4). Here, we discuss again some convergence issues before going to the final results for the vibrational density of states, which have been analyzed with respect to oxygen-related features and their displacement patterns. Finally, we summarize and draw a conclusion.

## 2. Method

All calculations have been carried out with the ABINIT package [7]. It is based on a plane-wave pseudopotential approach to the density-functional theory (DFT) [8, 9]. We have employed norm-conserving pseudopotentials in the Troullier-Martins style [10]. The exchange-correlation energy is described within the local-density approximation (LDA) [11, 12]. The phonon frequencies have been calculated utilizing the density-functional perturbation (DFPT) scheme [13, 14]. Since we apply a plane-wave method to an isolated systems we have used the supercell method and the  $\Gamma$  point only in the  $\mathbf{k}$  point sampling. The atomic positions have been relaxed till the residual forces have been less than 0.5 mHa/ $a_{\text{B}}$ .

## 3. Silan and Silanon

In a first step we have studied silan ( $\text{SiH}_4$ ) and silanon ( $\text{H}_2\text{SiO}$ ) as the smallest oxidized and non-oxidized silicon clusters. The atomic structure is shown in Fig. 1. Both systems are highly symmetric, with space groups  $T_d$  and  $C_{2v}$ , respectively. This yields in parts to a degeneracy of the vibrational frequencies.

The small molecules have been utilized for the convergence tests (Sect. 3.1), since the investigation of the big crystals is more time consuming. However, also the displacement patterns for the various vibrational modes have been analyzed (Sect. 3.2), and the resulting frequencies have been compared with reference values (Sect. 3.3).

### 3.1. Convergence tests

Applying a plane-wave approach together with a supercell method, the two main convergence parameters in the calculation are the kinetic-energy cutoff ( $E_{\text{cut}}$ ), which determines the number of plane waves used in the expansion, and the size of the (cubic) supercell, meaning the amount of vacuum around the isolated cluster. The latter parameter should be chosen as small as possible in order to reduce the computational effort, but large enough in order to avoid an interaction of the neighboring clusters, since periodic boundary conditions are employed.

The results for the variation of the total energy  $E_{\text{tot}}$  as a function of the of the supercell lattice parameter ( $a_{\text{cell}}$ ) and as a function of the  $E_{\text{cut}}$  are shown in Fig. 2. We have performed the convergence tests with respect to the  $E_{\text{cut}}$  for both silan and silanon, since the description of the oxygen requires a larger number of plane waves than for the other atoms. As visible in the figure, the size of the supercell has a rather small influence to the calculation. The variation of  $E_{\text{tot}}$  is in the  $\mu\text{Ha}$  range and therefore we have chosen  $a_{\text{cell}} = 30 a_{\text{B}}$ . The variation of  $E_{\text{tot}}$  with respect to the number of plane waves is larger. For silan convergence has been achieved at  $E_{\text{cut}} = 17.5 \text{ Ha}$  yielding an error of less than 0.4 mHa in  $E_{\text{tot}}$ . Compared with silan the total energy of silanon converges a factor of 10 slower. At  $E_{\text{cut}} = 32.5 \text{ Ha}$  we found a difference of less

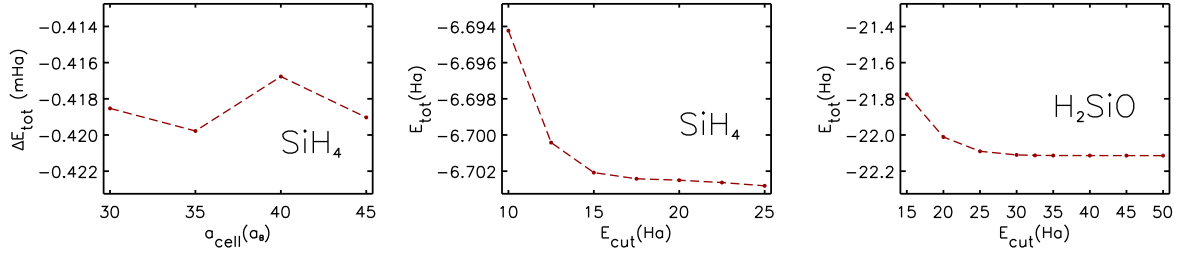


**Figure 2.** Total energy  $E_{\text{tot}}$  as a function of the supercell lattice parameter  $a_{\text{cell}}$  for silan (left), where the total energy is reduced by an offset of 6702 mHa, as a function of the kinetic energy cutoff  $E_{\text{cut}}$  for silan (middle) and silanon (right). Note that the scale of the total energy in the left figure is in mHa, whereas the scale in the other two figures is in Ha.

than 1.5 mHa compared with the value of  $E_{\text{tot}}$  at absolute convergence. Thus,  $E_{\text{cut}} = 32.5$  Ha is sufficient for the numerical description of silanon.

Since we want to investigate the vibrational excitations we inspected also the frequencies of silan and silanon. The lowest six frequencies, the translational and rotational ones should vanish. Due to the numerical noise and incompleteness of the plane-wave basis set, these frequencies do not vanish exactly. However, in the case of silanon, which is less converged with respect to the number of plane waves, they have values less than  $18\text{cm}^{-1}$  which is sufficiently small. For silan they are even smaller.

### 3.2. Eigenvectors for silan and silanon

The vibrations of silan and silanon can be characterized by their displacement patterns. Silan has 15 vibrational modes where 6 are vanishing. Analyzing the frequencies, we found that the lowest frequency is threefold, the next twofold, and the highest threefold degenerated due to the symmetry of the system. The eigendisplacements are shown in Fig. 3. There are two scissor and two stretching patterns, where in each case there is a symmetric displacement and an asymmetric one.

For silanon we have in total 12 frequency eigenvalues, from these six are vanishing. The remaining six true vibrations show no degeneracy. As for silan we have inspected the eigenvectors of silanon which are displayed in Fig. 4. Besides the two scissor and the two stretching modes, there are two bending modes, where for one the displacement of the hydrogen atoms is in the x-y plane, and for the other it is in the z direction (Note: the x-y plane is defined as the plane of the planar molecule). Also here, we have found symmetric and asymmetric modes for the

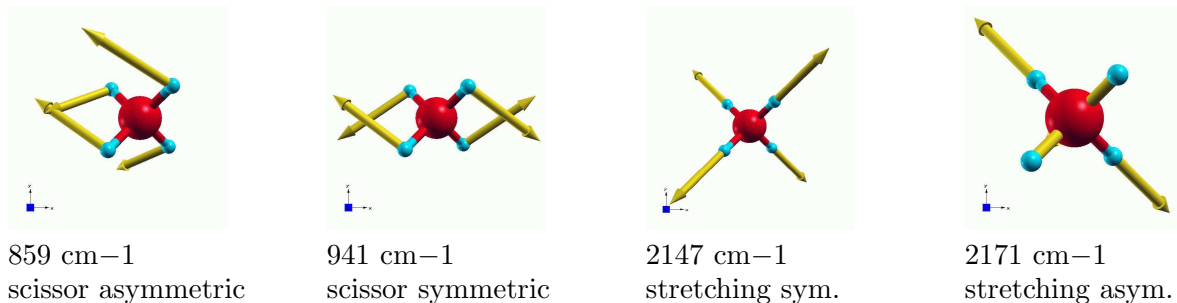


**Figure 3.** Eigenvectors of silan with symmetric (sym) and asymmetric (asym) displacements for the frequencies denoted in the subsets. For the assignment of the atoms see Fig. 1.

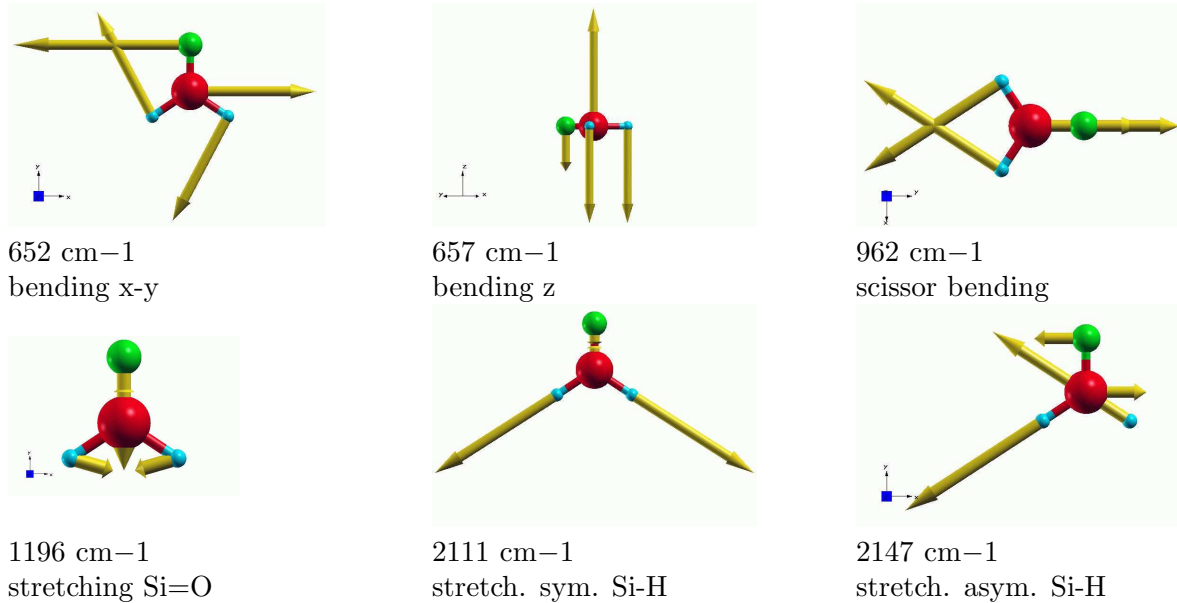


**Figure 4.** Eigenvectors of silanon with symmetric (sym) and asymmetric (asym) displacements for the frequencies denoted in the figures. The length of the oxygen- and silicon-related eigenvectors have been expanded for visibility. For the assignment of the atoms see Fig. 1

scissor and the stretching mode. The stretching modes can be divided in two classes: modes with a large movement of the oxygen and modes where the oxygen is displaced only a little. Usually the displacements of the hydrogens are at least a factor of 10 larger than the ones of the other atoms. Therefore, we have rescaled the eigenvectors of oxygen and silicon in the figure for visibility. There is just one mode where the displacement of the oxygen is in the same order of magnitude as the hydrogens: the stretching Si=O mode. This vibration mode is characteristic for the presence of oxygen in silanon.

### 3.3. Comparison with experimental results

For the small clusters silan and silanon there are experimental and theoretical reference data available to which we can compare our results. With this comparison we can also prove the

**Table 1.** Calculated bond distance and vibrational frequencies for silan in comparison with experimental results from of (a) Cadorna [15] and (b) Boyd [16] and theoretical tight-binding data.

Silan	this work	th [17]	th [18]	Experiment
Distance Si-H	1.4872 Å	1.48 Å	1.48 Å	1.4798 <sup>b</sup> Å
Frequencies (degeneracy):				
Scissor asym. (3)	859 cm <sup>-1</sup>	871 cm <sup>-1</sup>	831 cm <sup>-1</sup>	911 <sup>a</sup> cm <sup>-1</sup>
Scissor sym. H-Si-H (2)	941 cm <sup>-1</sup>	976 cm <sup>-1</sup>	984 cm <sup>-1</sup>	976 <sup>a</sup> cm <sup>-1</sup>
Stretching sym. H-Si (1)	2147 cm <sup>-1</sup>	2226 cm <sup>-1</sup>	2226 cm <sup>-1</sup>	2178 <sup>a</sup> cm <sup>-1</sup>
Stretching asym. H-Si (3)	2171 cm <sup>-1</sup>	2291 cm <sup>-1</sup>		2191 <sup>a</sup> cm <sup>-1</sup>

reliability of the computational approach used here.

A comparison of our results for silan with the measured data and available theoretical data is presented in Tab. 1. The overall agreement is good, however the experimental frequencies are slightly underestimated by the calculated ones. The relative difference between the results for the frequencies of Cardona [15] and ours is 6 % for the asymmetric scissor mode, 4 % for the symmetric one, 1 % for the symmetric and the asymmetric stretching mode. Besides, the agreement of the silicon-hydrogen bond length is excellent. For the lower frequencies the tight-binding results are more close to the experimental frequencies, however, these calculations used experimental values for the fitting of the tight-binding parameters whereas our calculation is fully ab initio.

For silanon there are just two experimental values available which have been obtained by infrared spectroscopy of silanon in an Ar matrix [19]: the silicon-oxygen stretching frequency at  $1202\text{ cm}^{-1}$  and a frequency at  $697\text{ cm}^{-1}$  where the assignment is not clear. It corresponds either to the bending frequency in x-y plane or to the one in the z direction. There exist theoretical investigations of the vibrational properties of silanon, based ab-initio approaches like molecular-orbital theory, Hartree-Fock, Configuration Interaction, Coupled-Cluster methods, and others [20–26]. In these calculations the results vary depending on the method, even sometimes within the same theoretical approach, e.g., just changing the basis set used in the local-orbital expansion. For example, the Si=O stretching frequency has been obtained at  $1355\text{ cm}^{-1}$  by Darling and Schlegel [22],  $1182\text{ cm}^{-1}$  by Gole and Dixon [21], and  $1217\text{ cm}^{-1}$  by Hargittai and Réffy [20] all by using the same molecular-orbital theory implementation in GAUSSIAN [27]. Thus, we have compared our results with some of the most recent theoretical values, which are the the molecular-orbital theory results using a B3LYP/6-311G(d,p) DFT basis set of Hargittai and Réffy [20], the molecular-orbital theory results using triple  $\zeta$  valence basis set at the local DFT level of Gole and Dixon [21], and the coupled cluster method results using quadruple  $\zeta$  basis set of Martin [24]. As visible in Tab. 2, the agreement with the theoretical references is very good. Therefore, the vibrational properties of isolated systems can be described very well using a periodic-cell approach based on plane waves instead on local orbitals. Inspecting the results more detailed, our results are very close to the ones of Gole and Dixon [21] also using a density-functional theory approach. Our results are in parts more close to the experimental values than the frequencies calculated by other groups.

**Table 2.** Calculated bond distances and vibrational frequencies for silanon in comparison with experimental (exp) results from Ref [28] (a) and Ref [19] (b) and theoretical (th) ones.

Silanon	this work	th. [20]	th. [21]	th. [24]	exp.
Distances (Å)					
Si-H	1.491	1.482	1.505	1.478	1.472 <sup>a</sup>
Si=O	1.505	1.517	1.534	1.522	1.515 <sup>a</sup>
Frequencies ( $\text{cm}^{-1}$ )					
Bending x-y plane	652	706	676	680	697 <sup>b</sup>
Bending z direction	657	712	693	692	
Scissor bending H-Si-H	962	1023	977	993	
Stretching Si=O	1196	1217	1197	1203	1202 <sup>b</sup>
Stretching sym. H-Si	2111	2223	2127	2162	
Stretching asym.H-Si	2140	2238	2132	2186	

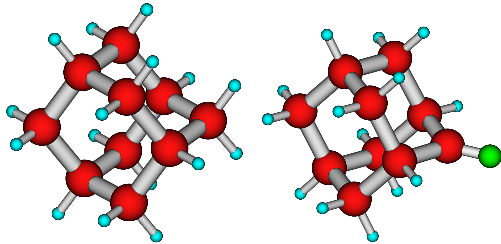


**Figure 5.**  $\text{Si}_{10}\text{H}_{16}$  (left) and  $\text{Si}_{10}\text{H}_{14}\text{O}$  (right). The assignment of the atoms is as in Fig. 1.

Last, we can compare the vibrations of silan with those of silanon. Here we found that the frequency of the Si-H-Si scissor-bending, the symmetric and the asymmetric Si-H modes in both systems have very similar frequencies which differ less than 2 % between silan and silanon. Thus, the intermediate Si=O stretching frequency can be utilized to characterize silanon experimentally.

#### 4. $\text{Si}_{10}\text{H}_{16}$ and $\text{Si}_{10}\text{H}_{14}\text{O}$

The big nanocrystals  $\text{Si}_{10}\text{H}_{16}$  and  $\text{Si}_{10}\text{H}_{14}\text{O}$  have been investigated in a similar way as the small ones.  $\text{Si}_{10}\text{H}_{16}$  has the same space group symmetry as silan. It is displayed in Fig. 5. In  $\text{Si}_{10}\text{H}_{16}$  there are two kinds of silicon atoms: those which are bonded to three other silicon atoms and which have therefore only one dangling bond which is saturated with a hydrogen atom, and those which are bonded to two other silicon atoms where two hydrogen atoms are necessary to saturate the bonds. There are various possibilities to oxidize this crystal. The oxygen can be bonded between first or second-neighbored silicon atoms, where each of the oxygen-bonding silicons will loose one hydrogen. However, we have chosen another configuration for  $\text{Si}_{10}\text{H}_{14}\text{O}$  (see Fig. 5) where the oxygen is double-bonded to a silicon atom yielding the same space group symmetry as silanon. Even if this configuration is not the energetically most favorable one, it is just  $\approx 60$  mHa less stable than the most stable one. Since  $\text{H}_2\text{SiO}$  and  $\text{Si}_{10}\text{H}_{14}\text{O}$  have both a double-bonded oxygen, one can compare the corresponding Si=O stretching frequencies.

Before investigating the vibrational properties of  $\text{Si}_{10}\text{H}_{16}$  and  $\text{Si}_{10}\text{H}_{14}\text{O}$  we want to reinspect the convergence parameters (Sect. 4.1). Afterwards, we analyze the vibrational density of states (Sect. 4.2) and the displacement patterns for oxygen-related modes (Sect. 4.3).

##### 4.1. Convergence

Since  $\text{Si}_{10}\text{H}_{16}$  and  $\text{Si}_{10}\text{H}_{14}\text{O}$  are larger than  $\text{SiH}_4$  and  $\text{H}_2\text{SiO}$  it is necessary to increase the size of the supercell from  $a_{\text{cell}} = 30 a_{\text{B}}$  for the small clusters to  $a_{\text{cell}} = 40 a_{\text{B}}$  for the big ones. With this choice, the kinetic-energy cutoff of  $E_{\text{cut}} = 17.5$  Ha can easily be used for the non-oxidized

**Table 3.** Variation of the vibrational frequencies in  $\text{cm}^{-1}$  of silanon for various values of the kinetic energy cutoff  $E_{\text{cut}}$ .

$E_{\text{cut}}$ (Ha)	15	20	25	30	32.5	35
Bending (x-y plane)	638	647	653	651	652	652
Bending (z dir.)	648	655	657	657	657	657
Scissor bending H-Si-H	960	961	962	961	962	962
Stretching Si=O	1150	1183	1195	1196	1196	1196
Stretching sym. H-Si	2109	2107	2110	2110	2111	2111
Stretching asym.H-Si	2137	2137	2140	2140	2140	2141

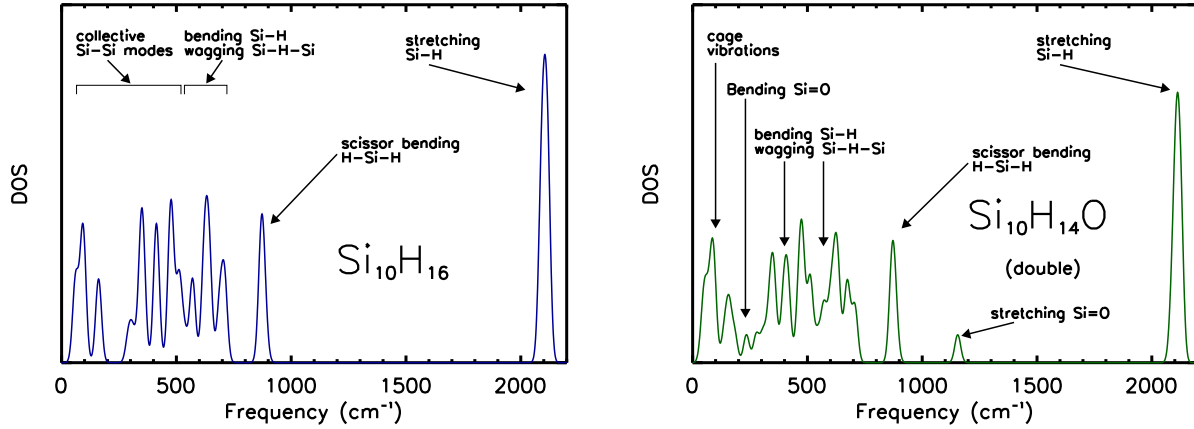


**Figure 6.** Vibrational density of states (DOS) of  $\text{Si}_{10}\text{H}_{16}$  (left) and  $\text{Si}_{10}\text{H}_{14}\text{O}$  (right) together with the assignment of the modes.

nanocrystal, whereas  $E_{\text{cut}} = 32.5$  Ha for the oxidized one is beyond the computational limits. Thus, we look at the vibrational frequencies for silanon as a function of  $E_{\text{cut}}$  (see Tab. 3). As noticed from the table, most of the frequencies do not vary significantly with the number of plane waves already from medium values of  $E_{\text{cut}}$ . The largest variations are found for the stretching  $\text{Si}=\text{O}$  frequency. However, even this frequency is already converged at  $E_{\text{cut}} = 25$  Ha. Thus, we could reduce the kinetic energy cutoff for silanon without obtaining significantly different results. In order to see if this conclusion is also true for  $\text{Si}_{10}\text{H}_{14}\text{O}$ , we have calculated the vibrational spectra at  $E_{\text{cut}} = 15$  Ha and at  $E_{\text{cut}} = 25$  Ha. For the Stretching  $\text{Si}=\text{O}$  we have found a difference of  $52 \text{ cm}^{-1}$  between these two calculations, which is nearly the same as for silanon comparing the values at the same kinetic-energy cutoffs. Since the other frequencies of  $\text{Si}_{10}\text{H}_{14}\text{O}$  did not vary significantly between the calculations using  $E_{\text{cut}} = 15$  Ha and  $E_{\text{cut}} = 25$  Ha, we can assume that convergence has been achieved at 25 Ha. This finding was confirmed, since the vanishing frequencies are lower than  $16 \text{ cm}^{-1}$ .

#### 4.2. Vibrational density of states

For the big nanocrystals we obtained a large number of frequencies. In the case of  $\text{Si}_{10}\text{H}_{16}$  we have found 78 frequency eigenvalues, where 6 frequencies vanish. However, most of the modes are twofold or threefold degenerated. For  $\text{Si}_{10}\text{H}_{14}\text{O}$  there are 75 frequencies and non of them is degenerated. Thus, we have calculated the vibrational density of states (DOS), where we applied a Gaussian broadening of a width of  $12.8 \text{ cm}^{-1}$ . The result is presented in Fig. 6. To our knowledge, there are no experimental data available for comparison for these two clusters.

Analyzing the DOS for  $\text{Si}_{10}\text{H}_{16}$ , we can distinguish four regions: the low-frequency collective  $\text{Si-Si}$  modes with frequencies up to  $\approx 500 \text{ cm}^{-1}$ , from  $\approx 500 \text{ cm}^{-1}$  to  $\approx 750 \text{ cm}^{-1}$  the  $\text{Si-H-Si}$  bending and wagging modes, the peak at  $\approx 870 \text{ cm}^{-1}$  corresponds to the  $\text{Si-H-Si}$  scissor-bending modes, and at  $\approx 2100 \text{ cm}^{-1}$  we have the  $\text{Si-H}$  stretching modes. Compared to silan, the  $\text{Si-H}$  stretching modes have slightly lower frequencies.

In the DOS of  $\text{Si}_{10}\text{H}_{14}\text{O}$  we find the same regions for the  $\text{Si}$  and  $\text{Si-H}$  related vibrations. In addition, we find in the frequency gaps some oxygen-related vibrations: at  $234 \text{ cm}^{-1}$  a  $\text{Si}=\text{O}$  bending mode and at  $1155 \text{ cm}^{-1}$  the  $\text{Si}=\text{O}$  stretching mode. These peaks in the DOS are the oxygen-signature in the spectra. The  $\text{Si}=\text{O}$  stretching frequency is comparable to that of silanon, which was at  $1196 \text{ cm}^{-1}$ . For the  $\text{Si}=\text{O}$  bending mode, the displacement of  $\text{Si}$  and  $\text{O}$  is similar to the bending  $x\text{-y}$  mode of silanon, however, it is at a quite different frequency.

We have compared also the DOS of  $\text{Si}_{10}\text{H}_{16}$  with the one of  $\text{Si}_{10}\text{H}_{14}\text{O}$ . Here we observe

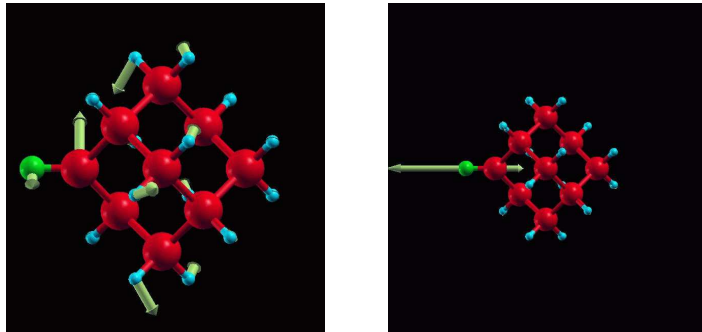


**Figure 7.** Eigendisplacements of oxygen-related modes, Si=O bending (left) and Si=O stretching (right) modes the frequencies  $234\text{ cm}^{-1}$  and  $1155\text{ cm}^{-1}$ , respectively.

that the peak of the Si-H stretching modes and the one of the Si-H-Si scissor-bending modes coincidence for both clusters and thus, they are independent of the presence of the oxygen. In contrary, the regions of the Si and Si-H related frequencies of  $\text{Si}_{10}\text{H}_{16}$  are slightly different from the ones of  $\text{Si}_{10}\text{H}_{14}\text{O}$ , since in the latter case there is an overlap with oxygen related modes. Nevertheless, it would be possible to discriminate experimentally the oxidized nanocrystals from the non-oxidized one due to the characteristic Si=O frequencies.

#### 4.3. Analysis of displacement patterns

After we have identified the characteristic oxygen-related spectral features in the DOS, we also want to analyze the displacement patterns of the corresponding modes. The eigenvectors of the Si=O bending and the Si=O stretching modes are displayed in Fig. 7. The Si=O bending mode has a delocalized character, where the Si=O stretching one is completely localized at the oxygen and its neighboring silicon atom. Both modes show no inversion symmetry and are Raman active.

### 5. Summary and outlook

We have investigated the silicon nanocrystals  $\text{SiH}_4$  (silan),  $\text{H}_2\text{SiO}$  (silanon),  $\text{Si}_{10}\text{H}_{16}$ , and  $\text{Si}_{10}\text{H}_{14}\text{O}$  with respect to their vibrational properties. The vibrational frequencies of silan and silanon are in good agreement with experimental and theoretical reference data. This shows, that localized systems like nanocrystals are well described using a plane-wave approach within periodic-boundary conditions. We have computed the vibrational density of states for the non-oxidized  $\text{Si}_{10}\text{H}_{16}$  and the corresponding oxidized one  $\text{Si}_{10}\text{H}_{14}\text{O}$  where the oxygen is double-bonded to a silicon atom. The frequencies have been analyzed with respect to their vibrational character. For  $\text{Si}_{10}\text{H}_{16}$  we have found four regions related to Si-Si vibrations and various Si-H motions. The same regions are present also in the density of states of  $\text{Si}_{10}\text{H}_{14}\text{O}$  cluster, where we have found additional peaks in the frequency gaps of  $\text{Si}_{10}\text{H}_{16}$ . These additional peaks have been identified as a non-localized Si=O bending mode and a localized Si=O stretching mode. Thus, comparing the vibrational density of states of the oxidized and the non-oxidized nanocrystal, we find a clear signature of the oxygen in the spectra.

A further investigation of these nanocrystals will contain an analysis of the vibrational spectra of other  $\text{Si}_{10}\text{H}_{14}\text{O}$  isomers, as well as a characterization of localized and non-localized modes and their Raman activity.

### Acknowledgments

This work was funded in part by the EU's 6th Framework Programme through the NANOQUANTA Network of Excellence (NMP-4-CT-2004-500198). Computer facilities at CINECA granted by INFN (Project no. 643/2006) are gratefully acknowledged. We also like to thank Matteo Gatti, Stefano Ossicini, and Paolo Giannozzi for fruitful discussions.



## References

- [1] Canham L T 1990 *Appl. Phys. Lett.* **57** 1046
- [2] Gatti M and Onida G 2005 *Phys. Rev. B* **72** 033313
- [3] Luppi M and Ossicini S 2003 *J. Appl. Phys.* **94** 2130
- [4] Luppi M and Ossicini S 2003 *Phys. Stat. Sol. (a)* **197** 251
- [5] Ossicini S, Iori F, Degoli E, Luppi E, Magri R, Poli R, Cantele G, Trani F and Ninno D 2006 *IEEE Journal of Selected Topics in Quantum Electronics* **12** 1585
- [6] Sychugov I, Juhasz R, Valenta J and Linnros J 2005 *Phys. Rev. Lett.* **94** 087405
- [7] <http://www.abinit.org>
- [8] Hohenberg P and Kohn W 1964 *Phys. Rev.* **136 B** 864
- [9] Kohn W and Sham L J 1965 *Phys. Rev.* **140 A** 1133
- [10] Troullier N and Martins J L 1991 *Phys. Rev. B* **43** 1993
- [11] Perdew J P and Zunger A 1981 *Phys. Rev. B* **23** 5048
- [12] Ceperley D M and Alder B J 1980 *Phys. Rev. Lett.* **45** 566
- [13] Gonze X and Lee C 1997 *Phys. Rev. B* **55** 10355
- [14] Gonze X 1997 *Phys. Rev. B* **55** 10337
- [15] Cardona M 1983 *Phys. Status Solidi B* **118** 463
- [16] Boyd D C J 1955 *J. Chem. Phys.* **23** 922
- [17] Kim E, Lee Y H and Lee J M 1994 *J. Phys.: Condens. Matter* **6** 9561
- [18] Min B J, Lee Y H, Wang C Z, Chan C T and Ho K M 1992 *Phys. Rev. B* **45** 6839
- [19] Withnall R and Andrews L 1985 *J. Phys. Chem.* **89** 3261
- [20] Hargittai M and Réffy B 2004 *J. Phys. Chem. A* **108** 10194
- [21] Gole J L and Dixon D A 1998 *Phys. Rev. B* **57** 12002
- [22] Darling C L and Schlegel H B 1993 *J. Phys. Chem* **97** 8207
- [23] Kudo T and Nagase S 1984 *J. Phys. Chem* **88** 2833
- [24] Martin J M L 1998 *J. Phys. Chem. A* **102** 1394
- [25] Ma B and Schaefer H F 1994 *J. Chem. Phys.* **101** 2734
- [26] Koput J, Carter S and Handy N C 1999 *Chem. Phys. Lett.* **301** 1
- [27] <http://www.gaussian.com>
- [28] Bogey M, Delcroix B, Walters A and Guillemin J C 1996 *J. Mol. Spectr.* **175** 421